

## ZEKE-PFI Spectroscopy of Benzocaine

Edurne Aguado, Asier Longarte, Estela Alejandro, José A. Fernández, and Fernando Castaño\*

Departamento de Química Física, Universidad del País Vasco, Apdo. 644, Bilbao 48080, Spain

Received: November 15, 2005

The adiabatic ionization threshold (AIT) of *trans*- and *gauche*-benzocaine has been measured by zero electron kinetic energy-pulsed field ionization (ZEKE-PFI) spectroscopy to be  $7.8412 \pm 0.0008$  eV (lasers at  $34134.4$  and  $29109.3$   $\text{cm}^{-1}$ ) and  $7.8421 \pm 0.0004$  eV ( $34144.8 + 29105.7$   $\text{cm}^{-1}$ ), respectively. AITs computed at the B3LYP/AUG-cc-p-VDZ level for the two conformers are some  $\sim 2500$   $\text{cm}^{-1}$  lower than the experimental; in contrast their energy difference is very close. The *trans*-benzocaine cation ZEKE spectra has been recorded taking a number of  $S_1$  intermediate vibronic states. The spectra provide an energy threshold for the appearance of intramolecular vibrational redistribution (IVR) around  $\sim 540$   $\text{cm}^{-1}$  in the  $S_1$  state.

## I. Introduction

Ethyl-*p*-aminobenzoate molecule (benzocaine) is a local anesthetic that inhibits the propagation of action potentials in excitable tissues by blocking the voltage-gated  $\text{Na}^+$  channels.<sup>1</sup> Since the affinity of the molecule for the receptor is closely related to the propensity to dock into the active site, a fine knowledge of the structure is needed to understand its function. The spectroscopy of benzocaine and some of its van der Waals clusters has been the subject of interest in a number of studies,<sup>2–8</sup> that have shown the existence of two conformers of rather similar stability. The position of the ethyl group relative to the aromatic ring in the *anti* and *gauche* benzocaine leads to an energy difference of  $\sim 150$   $\text{cm}^{-1}$ , as computed at the B3LYP/AUG-cc-pVDZ level. It is also worth noting that the title molecule belongs to a family of push–pull molecules with twisted intramolecular charge transfer (TICT).<sup>9–11</sup> However, the effect is not directly observed in benzocaine itself because the energy separation between the  ${}^1L_a$  and  ${}^1L_b$  electronic states is too large for molecules with no substituents in the amino group.

Despite the good understanding of the structure and spectroscopy of the benzocaine  $S_0$  and  $S_1$  states, to the best of our knowledge, no studies have been reported on the ion. This gap in the information prompted us to accomplish a zero electron kinetic energy-pulsed field ionization spectroscopy (ZEKE-PFI) study. ZEKE spectroscopy was developed in 1984<sup>12</sup> as a refinement of the photoelectron spectroscopy and it is grounded on the long lifetime of the Rydberg states with high  $n$  and  $l$  quantum numbers, the so-called molecular ZEKE states.<sup>13,14</sup> In conventional photoelectron spectroscopy, the molecular absorption of a high energy ionization photon yields (ions and) electrons whose excess energies are analyzed with a selector.<sup>15</sup> In contrast, in two-color ZEKE-PFI spectroscopy, two photons of appropriately selected tunable pump and probe lasers provide the energy and angular momentum to yield Rydberg states with high  $n$  and low  $l$  quantum states (2c-R2PI process). High-density Rydberg state species interacting with small stray fields mix their states producing long-lived high  $l$  and  $m_l$  states.<sup>16</sup> After a 300 ns–10  $\mu\text{s}$  delay, a few volts extraction pulse is applied, ionizing the high Rydberg states and driving the ZEKE electrons

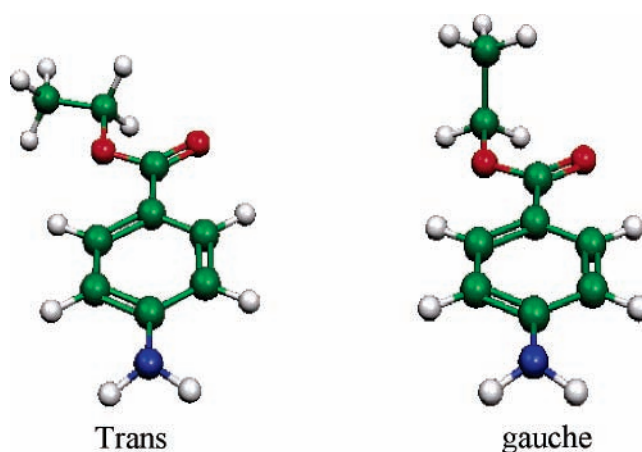


Figure 1. Ball and stick structures of the *trans* and *gauche* benzocaine conformers.

toward a detector. If the energy provided by the lasers is just over that of ionization threshold (IT) the energy excess appears as kinetic energy (energy and momentum conservation) and the low mass electrons escape from the extraction region before the pulse is applied and, hence, are no longer detected. The method yields the spectrum of the cation ground state with vibrational (and even rotational<sup>17</sup>) resolution, and the adiabatic ionization thresholds (AIT) are determined with very high accuracy.<sup>16</sup> Since its inception a considerable number of papers have been published,<sup>18</sup> despite the intrinsic difficulty and the frequent appearance of artifacts in the application.<sup>19</sup>

In the present paper we apply the ZEKE-PFI spectroscopy to determine the adiabatic ionization threshold (AIT) of the two benzocaine conformers. The rather small structure difference (Figure 1) leads to a mere  $4$   $\text{cm}^{-1}$  shift between their  $S_1 \leftarrow S_0$   $0_0^0$  transitions. The issue is to determine whether this difference is larger in the ion or not. Furthermore, there are studies that suggest that the B3LYP method is capable of qualitatively reproducing the shifts in AIT between conformational isomers of stable molecules and clusters. Therefore, the comparison between the experimental data and the DFT calculations will confirm or not such capability.

Finally, the use of a  $1 + 1'$  photon absorption process ionizes the molecules permitting one to record the ion spectra using a

\* To whom correspondence should be addressed. E-mail: f.castano@ehu.es. Telephone: +34 94 601 2533. Fax: +34 94 601 3500.

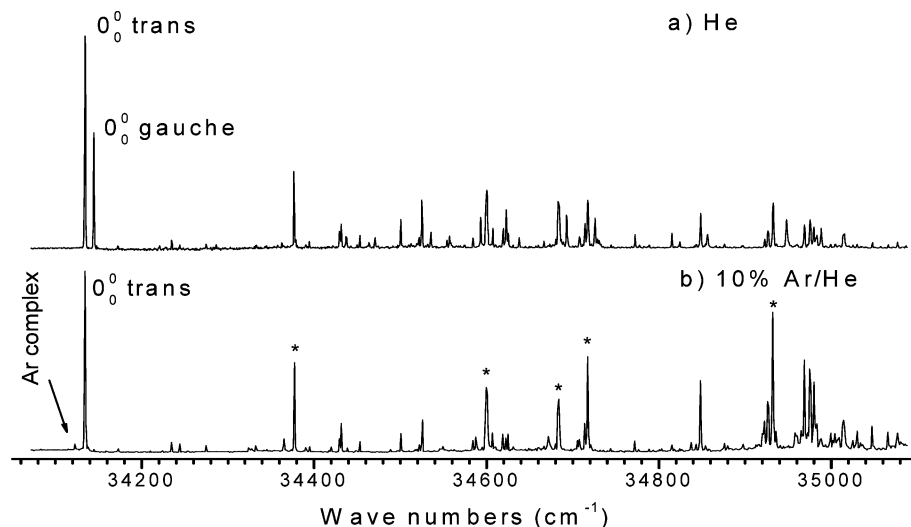


**Figure 2.** Two-color REMPI spectrum (R2PI) of a supersonic expansion of benzocaine in He at a stagnant pressure of 1.5 bar (a) and benzocaine in an He/(Ar 10%) mixture at 1.5 bar. The bands labeled with an asterisk have been employed as  $S_1$  intermediate vibronic states to monitor the ZEKE spectra (see Figure 7).

number of vibrational levels of the  $S_1$  electronic state. The method has been used to derive dynamic properties of the  $S_1$  state and, in particular, to determine the onset of the intramolecular vibrational redistribution (IVR).

## II. Experimental Setup

The experimental setup consists of a modified ZEKE-PFI spectrometer (built by R. M. Jordan Co, Inc. under request), equipped with two multichannel plate (MCP) detectors, for ions and for electrons respectively, two tunable pumping laser/dye laser/SHG coupled systems and the appropriate electronics for signal collecting, processing and further storage. A stainless steel pulsed valve (R. M. Jordan) was used to generate a supersonic beam expansion of a mixture of benzocaine vapor and either pure He or 10% Ar in He. Typical stagnation pressures were in the 2–5 bar range. Benzocaine was heated in an external oven to  $\sim 145$  °C (418 K) to get enough vapor pressure for the expansion mixture. As the Jordan valve is  $T$  limited to 90 °C (363 K), condensation appears in the valve nozzle and inside the stainless steel pipes. The tubes internal surface are covered with benzocaine, which is further heated, helping to maintain a concentration high enough to carry out the experiments.

The supersonic expansion is carried out inside the ZEKE spectrometer chamber, kept at an average working pressure of  $2 \times 10^{-5}$  mbar, and the central part of the plume is passed through an 1.0 mm  $\phi$  skimmer in order to get an improved uniform pulsed beam. The molecular expansion is crossed at right angles by an XeCl-excimer/dye laser beam, tuned at the benzocaine first electronic  $S_1$  state. A second laser, in a counter propagating coaxial geometry, overlapping spatially and temporally with the pump laser, ionizes the species with the minimum energy excess. A compact Lambda Physics Scanmate coupled to an in-house Quantel Brilliant B Nd:YAG laser was used as ionization laser.

Once the species of interest are ionized, the ions are accelerated by an electric field created by three parallel plates, V1, V2, and V3, set at  $4200 \pm 50$ ,  $3750 \pm 50$ , and 0 V and fly toward the MCP detector. The delayed arrival time is inversely proportional to the square root of the mass and the signal generated by the MCP is routed to a Tektronix TDS520 digital oscilloscope, where it is integrated, averaged, and sent to a PC computer for further analysis and storage.

In the ZEKE-PFI experiments plate V1 is set to ground. 800–1000 ns after the counterpropagating pump–probe pulsed lasers cross the expansion an extraction pulse of 3 V is applied to plate V2. The delay let time enough to the prompt electrons to fly away from the ionization region. The extraction pulse accelerates the ZEKE electrons out of the ionization region toward the detector and the ZEKE spectrum recorded by monitoring the field ionization yield as a function of the frequency of the second laser. The extraction voltage pulse was obtained from a digital function generator (Agilent 33250A).

The laser tuning was operated with Rhodamine 590, LDS 698, or DCM dyes (Exciton) and the laser wavelength was monitored in real time using a Wavemaster wavelength meter (Coherent).

## III. Theoretical Calculations

Theoretical calculations have been conducted to aid the assignment of the experimental spectra and to check if DFT methods provide sensible predictions of the AIT. All the calculations were conducted with the Gaussian 03<sup>20</sup> software in a cluster of PCs based on dual Athlon K7 (2000+) and P4 Xeon (2.4 GHz) processors. All the calculations are zero point energy corrected, unless specified otherwise. In the text, the vibrational modes of the aromatic ring are labeled using Wilson's nomenclature, while all the others are designed  $\nu_n$ , where  $n$  is a sequential vibration number, beginning with the lowest energy ( $\nu_1$  for the lowest,  $\nu_2$  for the next and so on).

## IV. Results and Discussion

The 2-color REMPI (R2PI) spectrum of benzocaine in a supersonic expansion is depicted in Figure 2a. The two intense bands of the spectrum are readily identified as the trans and gauche benzocaine  $0_0^0$  transitions.<sup>2</sup> The energy difference between the two conformers, computed to be  $\sim 150$   $\text{cm}^{-1}$  at the B3LYP/AUG-cc-pVDZ level, results in a  $0_0^0$  band intensities ratio of  $\sim 2:1$  (Figure 2a). However, if the supersonic expansion is carried out with a 10% Ar/He mixture, only the more stable conformer band is observed (Figure 2b). Usually, a deeper and faster cooling freezes down the less stable initial population, precluding the population transfer to the most stable species. In contrast, the observed species in our system is the most stable. It may well be that the collisions with the buffer gas are

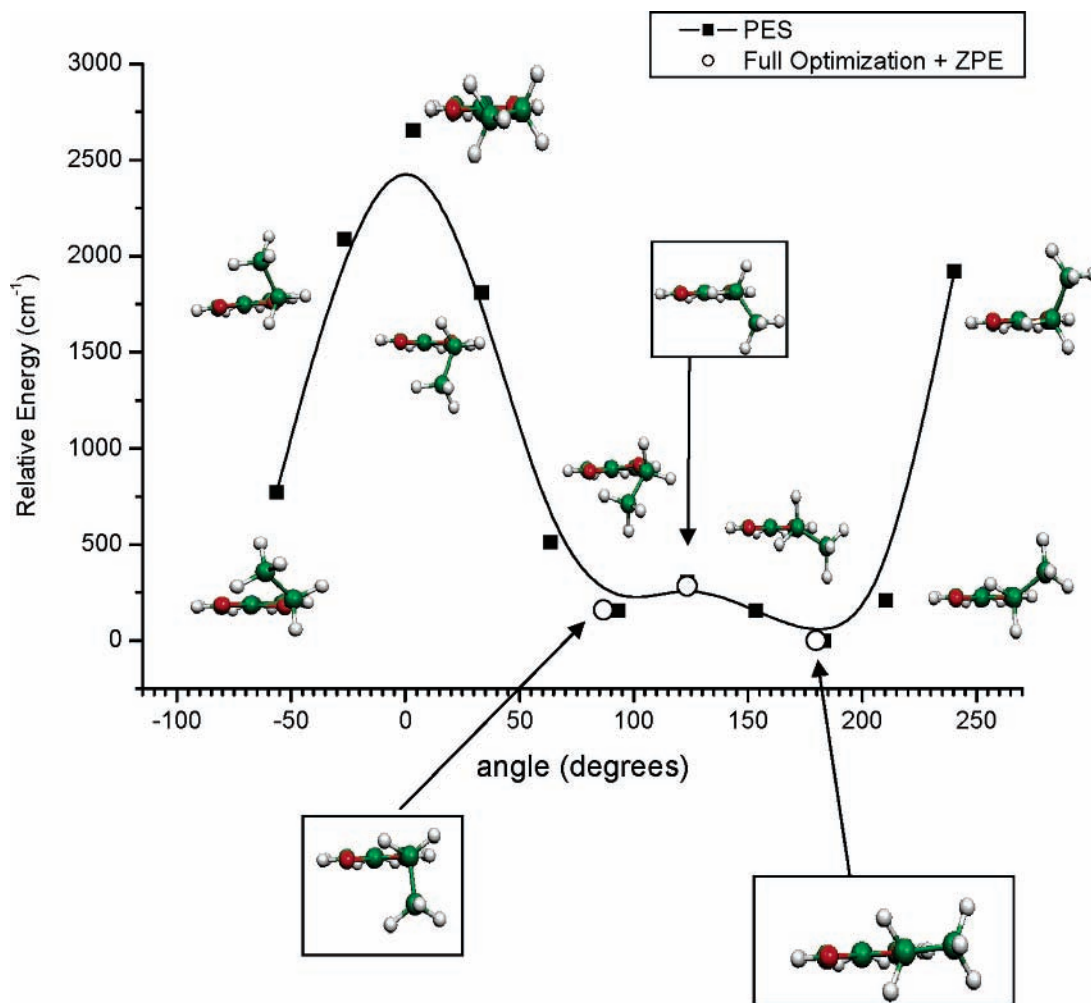


**Figure 3.** Relaxed potential energy profile of the rotation of the propyl group around the O-Et bond in benzocaine. The open circles stand by ZPE corrected full optimizations energies. The fit to the filled squares is a simple  $\beta$ -spline to draw the potential energy. Note the small energy barrier size of the isomerization process.

energetic enough to drive the population of the less stable isomer over the isomerization barrier into the more stable conformer. To substantiate the argument, an examination of the gauche–trans isomerization potential energy surface (PES) was carried out. Figure 3 shows a relaxed potential energy scan (RPES option in Gaussian) at the B3LYP/AUG-cc-pVDZ level. The open circles correspond to ZPE corrected full optimizations. The fit to the filled squares is a simple  $\beta$ -spline to sketch the potential energy. It should be noted that the barrier between gauche and trans conformers is less than about  $50\text{ cm}^{-1}$  and the collisions with Ar may involve enough energy to overcome the shallow barrier. Such a property has been used to record the ZEKE spectra of the trans species, without interferences from the gauche isomer.

The ZEKE spectra of both *trans*- and *gauche*-benzocaine, recorded using the  $S_1\ 0^0$  level as intermediate state, are shown in Figure 4, where the wavenumber scale corresponds to the energy of the ionization photon. Because of the large size and low symmetry of benzocaine, the vibration motions are strongly coupled. Wilson's nomenclature is used for the ring vibrations while other bands are labeled in order of ascending energy. For the gauche conformer a number of vibrational assignments are feasible and are tagged in Figure 4.

At first glance, the spectra of *trans*- and *gauche*-benzocaine look appreciably different. The spectrum of the trans conformer has a larger number of usually more intense bands than that of the gauche. The symmetry may be one argument to explain the

difference: the trans conformer belongs to the  $C_s$  symmetry group, with two irreducible representations  $A'$  and  $A''$  while the gauche conformer belongs to the  $C_1$  point group (with no symmetry operations other than the identity). The  $S_1$  and  $D_0$  states of trans benzocaine fit in  $A'$  and  $A''$  irreducible representations respectively;<sup>21</sup> similarly,  $\mu_x$  and  $\mu_y$  dipole moments belong to  $A'$  and the  $\mu_z$  dipole moment belongs to  $A''$ . Therefore, all the trans vibrations are electric dipole allowed within the  $D_0 \leftarrow S_1$  transition, although the vibrations with  $A''$  symmetry (for example, out of plane ring vibrations) are expected to be more intense, since  $\mu_x$  is the strongest component of the dipole moment. The gauche conformer, with no symmetry operations other than the identity, has all the electric dipole transitions allowed. An additional difference between the structure of the conformers is the relative orientation of the ethyl group and the aromatic moiety, giving rise to a significant degree of mixing of the aromatic ring and the ethyl group normal modes, that finally yields a shift of vibrational frequencies and a change in the intensity of the vibronic bands.

The AIT accuracy is noticeably improved by extrapolating the measurements at a series of extraction voltages.<sup>22</sup> In fact, the ionization threshold varies with the extraction electric field according to<sup>23</sup>

$$\frac{\Delta E}{hc(\text{cm}^{-1})} = k\sqrt{F/(\text{V}/\text{cm})}$$

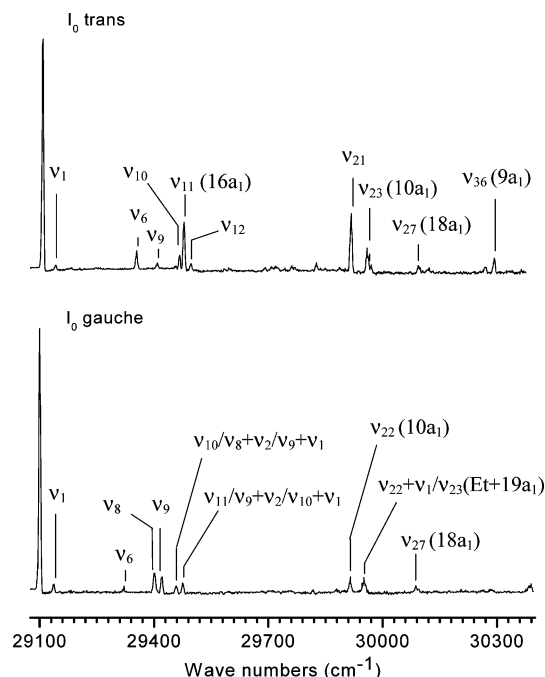


**Figure 4.** ZEKE-PFI spectra of *trans*-benzocaine (upper trace) and *gauche*-benzocaine (lower trace), recorded using the  $S_1$   $0^0$  level as intermediate state. The assignments of the significant vibrational bands are labeled. For some of them, more than one assignment is possible, and so it is indicated.

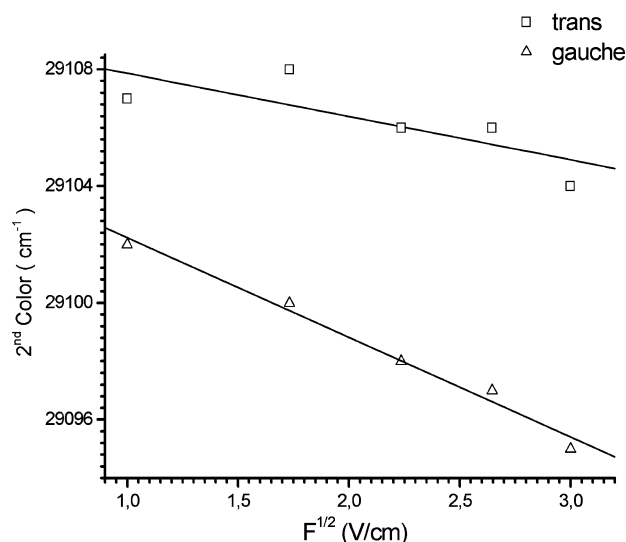


**Figure 5.** Adiabatic ionization thresholds vs extraction field voltages plots for *trans*- and *gauche*-benzocaine. Extrapolation to zero field yields appearance ionization total energies for the *trans* and *gauche* conformers of  $63244 \pm 6$  and  $63251 \pm 3$   $\text{cm}^{-1}$ .

where  $F$  is the applied electric field (V/cm), and  $k$  is a constant, known to be about 4 for diabatic and 6 for adiabatic field ionization processes. Figure 5 depicts the ionization onset of the  $D_0 \leftarrow S_1$  transition of the *gauche* and *trans* isomers as a function of the electric field applied  $F$ . Extrapolation to zero field yields the following ionization thresholds:  $7.8412 \pm 0.0008$  eV ( $34134 + 29109$   $\text{cm}^{-1}$ ) for *trans*-benzocaine, and  $7.8421 \pm 0.0004$  eV ( $34144 + 29105$   $\text{cm}^{-1}$ ) for *gauche*-benzocaine. Previously reported AIT using R2PI<sup>7</sup> differ from these values by ca. 30  $\text{cm}^{-1}$ . Table 1 compares the AIT of benzocaine with those of other aniline derivatives.

The difference of the AITs of aniline and benzocaine shows that the ester group induces a  $\sim 100$   $\text{cm}^{-1}$  blue shift to the  $S_1$

**TABLE 1: Comparison between Adiabatic Ionization Thresholds (AIT) of Some Aniline Derivatives (in Wavenumbers)**

molecule	$S_1 \leftarrow S_0$	$I_0 \leftarrow S_1$	AIP
aniline <sup>a</sup>	34 029	28 242	$62268 \pm 4$
<i>anti</i> <i>p-n</i> -propylaniline <sup>b</sup>	33 266	26 451	$59717 \pm 3$
<i>gauche</i> <i>p-n</i> -propylaniline <sup>b</sup>	33 211	26 582	$59793 \pm 3$
<i>trans</i> -benzocaine <sup>c</sup>	34 134	29 109	$63243.7 \pm 6^d$
<i>trans</i> -benzocaine, computed <sup>f</sup>			61 762
<i>gauche</i> -benzocaine <sup>c</sup>	34 145	29 106	$63250.5 \pm 3^e$
<i>gauche</i> -benzocaine, computed <sup>f</sup>			61 787

<sup>a</sup> From ref 27. <sup>b</sup> From ref 26. <sup>c</sup> This work. <sup>d</sup> Estimated from R2PI:  $63281 \pm 20$   $\text{cm}^{-1}$ . <sup>e</sup> Estimated from R2PI:  $63283 \pm 20$   $\text{cm}^{-1}$ . <sup>f</sup> At the B3LYP/AUG-cc-pVDZ level.

$\leftarrow S_0$  transition. However, the influence in the  $D_0 \leftarrow S_1$  transition energy is significantly larger,  $\sim 700$   $\text{cm}^{-1}$ . As the ester group induces a blue shift in the aniline chromophore, one concludes that the ester group is an electron-withdrawing substituent.

The influence of the orientation of the ethyl group on the electronic transition and on the AIP is very small: only 11  $\text{cm}^{-1}$  for the  $S_1 \leftarrow S_0$  transition and 7  $\text{cm}^{-1}$  for the  $D_0 \leftarrow S_1$ . These shifts are smaller than the corresponding shift in the AIT of the aniline derivatives conformers. For example, the *anti* and *gauche* conformers of *p-n*-propylaniline are separated 77  $\text{cm}^{-1}$  (Table 1). The larger difference is probably due to the direct interaction between the alkyl substituent and the aromatic ring in the *gauche-p-n*-propylaniline, which is not present in the *anti* isomer.

The AITs have been computed for optimized structures at the B3LYP/AUG-cc-pVDZ level and are compared with the experimental values in Table 1. It should be noted that although the calculated AITs are ca. 2500  $\text{cm}^{-1}$  smaller than those measured, the calculations correctly predict a higher AIT for the *gauche* conformer. The predictive power of the B3LYP method has been previously employed for molecules of the same size,<sup>24</sup> showing that this calculation level always yield values that are  $\sim 2000$   $\text{cm}^{-1}$  too low, although it is able to predict differences between isomer's AITs. In the present case, due to the small difference between AITs, the good agreement between experimental and calculated energies might be accidental.

To obtain dynamic information on the  $S_1$  excited state, the ZEKE spectra of the *trans* conformer were measured using a few vibrational levels of the  $S_1$  state, labeled with asterisks in Figure 2b and depicted in Figure 6. The  $S_1$   $\nu_6$  and  $9b$  modes includes skeletal motions of the ethyl ester group. As expected by symmetry, in plane (*ip*) and out of plane (*oop*) vibrations are observed.

Figure 7 shows the ZEKE-PFI spectra obtained using intermediates  $S_1 0_0^0$ ,  $S_1 \nu_6^1$ ,  $S_1 9b^1$ ,  $S_1 6a^1$ ,  $S_1 6b^1$ , and  $S_1 10a^1$  vibronic states, at 0, 242, 466, 548, 583, and 798  $\text{cm}^{-1}$  respectively over the  $0_0^0$  transition. To ensure that no transitions from the *gauche* conformer are excited and to maximize the *trans* population, and therefore the signal intensity, a 10% Ar/He mixture was employed as stagnant gas. Note that the gray region in the upper three spectra shows the blind area of our BBQ crystal. The assignments shown in Figure 7 are based on the comparison between the normal modes computed at the B3LYP/AUG-cc-pVDZ level and the experimental band energies.

In the case of the  $S_1 \nu_6^1$  intermediate vibronic state, the ZEKE spectra show a progression with three bands. Some other weak features, labeled as  $16a_1^+$ ,  $6b_1^+$ , and  $\nu_6 + \nu_{21}^+$  are also observed. A similar pattern is observed for the  $S_1 9b^1$  state, although with an increase in the vibrational activity: most of the vibrational

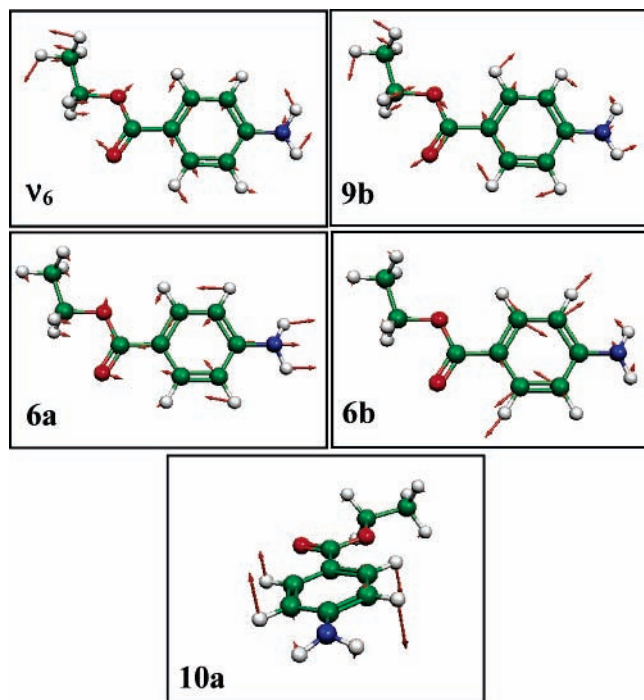


**Figure 6.** Vibrational motion drawings of the  $S_1$  intermediate vibronic states used for recording the ZEKE-PFI spectra of *trans*-benzocaine (Figure 9).

activity is related to the  $9b_1^+$  combination bands. At lower energy, only the ethyl group  $\nu_2$  vibration is barely identified. (A detailed description of the normal modes of the species studied in the paper is available upon request from the authors.) The ph-COOEt stretching  $\nu_9$  vibration is also very active.

A considerably different picture is observed if  $S_1$   $6a^1$  ( $548\text{ cm}^{-1}$ ) is taken as the intermediate state. In addition to the very low intensity  $\nu_5$  and  $\nu_6$  bands at low energies, a strong band at  $535\text{ cm}^{-1}$  comes out, assigned to  $16b_1^+$ , and another at  $601\text{ cm}^{-1}$  is associated with  $6a_1^+$ . The last band has a number of shoulders. Apparently, the close  $6a^1$  and  $16b^1$  normal modes (separated by  $16\text{ cm}^{-1}$ ) are highly coupled in the  $S_1$  state. Most likely, the coupling takes place through the ethyl group vibrations (Figure 2). Also a small band to the blue of the  $6a_1^+$  is identified as the  $6b_1^+$ .

Two additional features were identified in the spectrum with  $S_1$   $6a^1$  as intermediate state; assigned to  $16b_1^+$  combination bands. The low-intensity background extending along the spectrum suggests that an intramolecular vibrational energy redistribution (IVR) is taking place in the  $S_1$  state. The background increases in intensity when higher energy vibrations are used as intermediate states. For example, for the  $S_1$   $6b^1$  state, three bands over an intense background become visible. Of these bands, the highest energy one is identified as the  $6b_1^+$ ; not far from it is the  $6a_1^+$  and a lower energy band that is difficult to identify. With the aid of the computed normal modes at the UB3LYP/AUG-cc-pVDZ level, the band is assigned to the torsion of the ph-NH<sub>2</sub> bond ( $\rho_t(\text{NH}_2)$ ). However, the band appears at much lower energy in the  $S_1$  state, and therefore, it is very unlikely to be coupled to the  $6b^1$  mode. Certainly the assignment is tentative, because it only relies on the comparison with the DFT calculation.

The upper-most spectrum in Figure 7 is obtained with the  $S_1$   $10a^1$  ( $798\text{ cm}^{-1}$ ) vibronic level as intermediate state. It includes a vertical transition and a broadband absorption. Also  $D_0$  is present with very low intensity. No significant increase of the background has been observed.

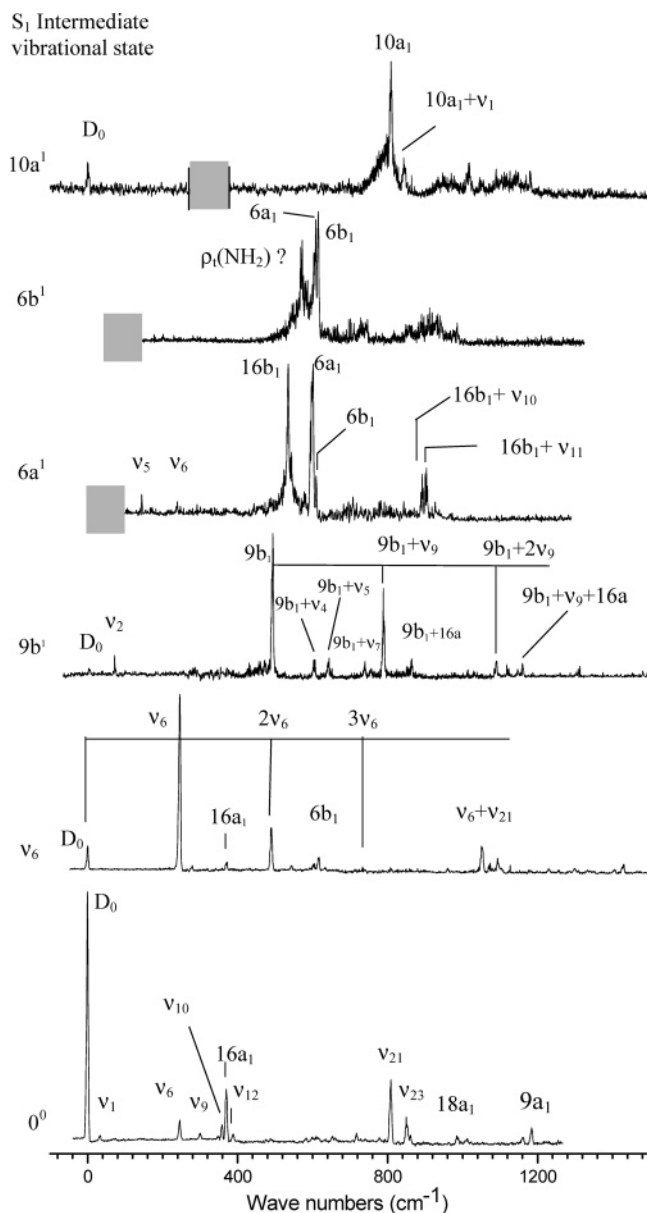


**Figure 7.** ZEKE-PFI spectra of *trans*-benzocaine recorded using  $S_1$   $0^0$ ,  $S_1$   $\nu_6^1$ ,  $S_1$   $9b^1$ ,  $S_1$   $6a^1$ ,  $S_1$   $6b^1$ , and  $S_1$   $10a^1$  as intermediate states. The assignment of some significant bands are labeled. The gray region of the spectra is a blind region of our BBQ crystal.

As mentioned above, a plausible explanation for the appearance of an intense background is the presence of an IVR process. Some authors have described similar behavior for *p-n*-propylphenol<sup>25</sup> and *p-n*-propylaniline.<sup>26</sup> Li et al. reported that the transition through  $S_1$   $1^1$  intermediate state in the MATI spectrum of *trans p-n*-propylphenol cation results in a broadband absorption extending over ca.  $1500\text{ cm}^{-1}$  and several resolved transitions. However, the same spectrum, but recorded using any other  $S_1$  vibronic level with less internal energy as intermediate yielded a well resolved spectrum. They concluded that the *p-n*-propylphenol has an IVR upper limit at  $810\text{ cm}^{-1}$ , i.e., close to the energy of the mentioned vibration. Similarly, the lower energy  $S_1$  vibronic state that yields a broad spectrum in *trans* benzocaine is located  $548\text{ cm}^{-1}$  above the origin, and the change in shape of the spectra using  $S_1$  vibronic states above and below the mentioned vibronic level is not as severe as in ref 25.

It is expected that *p-n*-propylaniline has a closer behavior to benzocaine than *p-n*-propylphenol. Song et al.<sup>26</sup> performed a

spectroscopic study of the anti and gauche *p-n*-propylaniline cation conformers, using several  $S_1$  intermediate states. All the spectra have sharp features, but those recorded with  $S_1 D_0^2$  as intermediate state, with  $1247\text{ cm}^{-1}$  vibrational energy, have broadband absorptions and some sharp features. Furthermore, the anti conformer background is less intense than that for the gauche. It is worth noting that the anti conformer of the *p-n*-propylaniline has the propyl group pointing away from the ring, while in the gauche conformer it is folded back and interacts with the ring. The mentioned interactions mix the vibronic states to a different extent, leading to a faster IVR for the gauche conformer.

The arguments can be extrapolated to the present case, where the trans conformer has the ethyl group in the plane of the aromatic ring, favoring the coupling between ring and alkyl normal modes. Thereby a vibrational energy excess of  $\approx 550\text{ cm}^{-1}$  is required to trigger the IVR process. Unfortunately, the weak signal of the gauche benzocaine precludes obtaining spectra with other intermediate states other than the  $0^0$  band. The experiment would confirm the hypotheses of the coupling by the ethyl vibrational modes, since in the gauche conformer the ethyl group is out of the molecular plane.

## V. Conclusions

A determination of the *trans*- and *gauche*-benzocaine adiabatic ionization thresholds has been conducted by ZEKE-PFI spectroscopy, yielding  $7.8412 \pm 0.0008\text{ eV}$  ( $34134.4 + 29109.3\text{ cm}^{-1}$ ) and  $7.8421 \pm 0.0004\text{ eV}$  ( $34144.8 + 29105.7\text{ cm}^{-1}$ ), respectively. It is concluded that the ester substituent behaves as an electron-withdrawer and that the orientation of the ethyl group has little influence on the AIT. The very small ionization energy difference between the conformers may be attributed to the zero-point vibrational energy.

Calculations for both conformers conducted at the B3LYP/AUG-cc-pVDZ level yield AITs  $\sim 2500\text{ cm}^{-1}$  lower than those determined by ZEKE. However, the computations correctly predict the *trans*- and *gauche*-benzocaine relative ionization energies. The capability of the B3LYP method to correctly predict relative AITs of these conformers has been demonstrated for similar molecules,<sup>24</sup> although for the small differences in *trans*- and *gauche*-benzocaine, the agreement might be accidental.

The *trans*-benzocaine cation spectra have been obtained with a number of intermediate  $S_1$  vibronic states. The spectra have sharp well resolved features for intermediate levels with energies below  $\sim 540\text{ cm}^{-1}$ . Spectra with high vibrational energy intermediate states show a broad background presumably due to the redistribution of the vibrational energy. The low energy threshold for the IVR is argued to be a consequence of the coupling between the ethyl and the aromatic ring vibrations.

**Acknowledgment.** The authors are grateful to MEC and MCYT (Madrid) for partial support of this work through Grants BQU2001-0511 and CTQ2004-07188/BQU, to GV (Vitoria) and to UPV for a Consolidated Research Group Grant (2001-05), and to Consejería de Industria of the GV (Vitoria) for two Eortek Grants. E.A. thanks the UPV and the Spectroscopy Group for a Fellowship Associated to Project.

## References and Notes

- (1) Godwin, S. A.; Cox, J. R.; Wright, S. N. *Biophys. Chem.* **2005**, *113*, 1.
- (2) Howells, B. D.; McCombie, J.; Palmer, T. F.; Simons, J. P.; Walters, A. J. *Chem. Soc., Faraday Trans.* **1992**, *88*, 2595. Howells, B. D.; McCombie, J.; Palmer, T. F.; Simons, J. P.; Walters, A. J. *Chem. Soc., Faraday Trans.* **1992**, *88*, 2603.
- (3) Pereira, R.; Álava, I.; Castaño, F.; Martínez, M. T. *J. Chem. Soc., Faraday Trans.* **1994**, *90*, 2443.
- (4) Pereira, R.; Calvo, T.; Castaño, F.; Martínez, M. T. *Chem. Phys.* **1995**, *201*, 433.
- (5) Hepworth, P. A.; McCombie, J.; Simons, J. P.; Pfanstiel, J. F.; Ribblet, J. W.; Pratt, D. W. *Chem. Phys. Lett.* **1996**, *249*, 341.
- (6) Ribblet, J. W.; Sinclair, W. E.; Pratt, D. W. *Isr. J. Chem.* **1997**, *37*, 395.
- (7) Longarte, A.; Fernández, J. A.; Unamuno, I.; Castaño, F. *Chem. Phys. Lett.* **2000**, *260*, 83.
- (8) Fernández, J. A.; Longarte, A.; Unamuno, I.; Castaño, F. *J. Chem. Phys.* **2000**, *113*, 8531.
- (9) Grabowski, Z. R.; Rotkiewicz, K.; Siemiarz, A.; Cowley, D. J.; Baumann, W. *Nouv. J. Chem.* **1979**, *3*, 443.
- (10) Rettig, W.; Wermuth, G.; Lippert, E. *Ber. Bunsen-Ges. Phys. Chem.* **1979**, *83*, 692.
- (11) Herbich, J.; Salgado, F. P.; Rettschnick, R. P. H.; Grabowski, Z. R.; Wojtowicz, H. J. *Phys. Chem.* **1991**, *95*, 3491.
- (12) Müller-Dethlefs, K.; Sander, M.; Schlag, E. W. *Z. Naturforsch. A* **1984**, *39*, 1089.
- (13) Cockett, M. R. C.; Donovan, R. J.; Lawley, K. P. *J. Chem. Phys.* **1996**, *105*, 3347.
- (14) Müller-Dethlefs, K.; Schlag, E. W. *Annu. Rev. Phys. Chem.* **1991**, *42*, 109.
- (15) Ballard, R. E. *Photoelectron Spectroscopy and Molecular Orbital Theory*; K. Hilger: Bristol, U.K., 1978.
- (16) Schlag, E. W. *ZEKE spectroscopy*; Cambridge University Press: Cambridge, U.K., 1998.
- (17) Neusser, N. H.; Siglow, K. *Chem. Rev.* **2000**, *100*, 3921.
- (18) Dessent, C. E. H.; Müller-Dethlefs, K. *Chem. Rev.* **2000**, *100*, 3999 and references therein.
- (19) Signorell, R.; Merkt, F. Artifacts in PFI-ZEKE photoelectron spectroscopy. In *The role of Rydberg states in Spectroscopy and Photochemistry*; Sándorfy, C., Ed.; Kluwer Academic Publishers: Amsterdam, 1999.
- (20) *Gaussian 03, Revision B.04*. Frisch, M. J.; Trucks, G. W.; Schlegel, H. B.; Scuseria, G. E.; Robb, M. A.; Cheeseman, J. R.; Montgomery, J. A., Jr.; T. Vreven, T.; K. N. Kudin, K. N.; Burant, J. C.; Millam, J. M.; Iyengar, S. S.; Tomasi, J.; Barone, V.; Mennucci, B.; Cossi, M.; Scalmani, G.; Rega, N.; Petersson, G. A.; Nakatsuji, N.; Hada, M.; Ehara, M.; Toyota, K.; Fukuda, R.; Hasegawa, J.; Ishida, M.; Nakajima, T.; Honda, Y.; Kitao, O.; Nakai, H.; Klene, M.; Li, X.; Knox, J. E.; Hratchian, H. P.; Cross, J. B.; Adamo, C.; Jaramillo, J.; Gomperts, R.; Stratmann, R. E.; Yazyev, O.; Austin, A. J.; Cammi, R.; Pomelli, C.; Ochterski, J. W.; Ayala, P. Y.; Morokuma, K.; Voth, G. A.; Salvador, P.; Dannenberg, J. J.; Zakrzewski, V. G.; Dapprich, S.; Daniels, A. D.; Strain, M. C.; Farkas, O.; Malick, D. K.; Rabuck, A. D.; Raghavachari, K.; Foresman, J. B.; Ortiz, J. V.; Cui, Q.; Baboul, A. G.; Clifford, S.; Cioslowski, J.; Stefanov, B. B.; Liu, G.; Liashenko, A.; Piskorz, P.; Komaromi, I.; Martin, R. L.; Fox, D. J.; Keith, T.; Al-Laham, M. A.; Peng, C. Y.; Nanayakkara, A.; Challacombe, M.; Gill, P. M. W.; Johnson, B.; Chen, W.; Wong, M. W.; Gonzalez, C.; Pople, J. A. Gaussian, Inc.: Pittsburgh, PA, 2003.
- (21) Bunker, P. R.; Jensen, P. *Fundamentals of Molecular Symmetry*; Series in Chemical Physics; Institute of Physics: Bristol, 2005.
- (22) Kleppner, D.; Littman, M. G.; Zimmerman, M. L. In *Rydberg States of Atoms and Molecules*; Stebbings, R. F., Dunning, F. B. Eds.; Cambridge University Press: New York, 1983.
- (23) Gallagher, T. F. *Rydberg Atoms*; Cambridge University Press: Cambridge, U.K., 1994.
- (24) Alejandro, E.; Fernández, J. A.; Castaño, F. *Chem. Phys. Lett.* **2002**, *353*, 195 and references therein.
- (25) Li, C.; Lin, J. L.; Tzeng, W. B. *J. Chem. Phys.* **2005**, *122*, 44311.
- (26) Song, X.; Davidson, E. R.; Gwaltney, S. R.; Reilly, J. P. *J. Chem. Phys.* **1994**, *100*, 5411.
- (27) Takahashi, M.; Ozeki, H.; Kimura, K. *J. Chem. Phys.* **1992**, *96*, 6399.